2014

Characterization of acyl chain position in unsaturated phosphatidylcholines using differential mobility-mass spectrometry

Alan Maccarone
University of Wollongong, alanmac@uow.edu.au

Jackson Duldig
University of Wollongong, jd705@uowmail.edu.au

Todd W. Mitchell
University of Wollongong, toddm@uow.edu.au

Stephen J. Blanksby
Queensland University of Technology, blanksby@uow.edu.au

Eva Duchoslav
AB SCIEX

See next page for additional authors

Publication Details

Maccarone, A. T., Duldig, J., Mitchell, T. W., Blanksby, S. J., Duchoslav, E. & Campbell, J. Larry. (2014). Characterization of acyl chain position in unsaturated phosphatidylcholines using differential mobility-mass spectrometry. Journal of Lipid Research, 55 (8), 1668-1677.

Characterization of acyl chain position in unsaturated phosphatidylcholines using differential mobility-mass spectrometry

Abstract
Glycerophospholipids (GPs) that differ in the relative position of the two fatty acyl chains on the glycerol backbone (i.e., sn-positional isomers) can have distinct physicochemical properties. The unambiguous assignment of acyl chain position to an individual GP represents a significant analytical challenge. Here we describe a workflow where phosphatidylcholines (PCs) are subjected to ESI for characterization by a combination of differential mobility spectrometry and MS (DMS-MS). When infused as a mixture, ions formed from silver adduction of each phospholipid isomer {e.g., [PC (16:0/18:1) + Ag]+ and [PC (18:1/16:0) + Ag]+} are transmitted through the DMS device at discrete compensation voltages. Varying their relative amounts allows facile and unambiguous assignment of the sn-positions of the fatty acyl chains for each isomer. Integration of the well-resolved ion populations provides a rapid method (< 3 min) for relative quantification of these lipid isomers. The DMS-MS results show excellent agreement with established, but time-consuming, enzymatic approaches and also provide superior accuracy to methods that rely on MS alone. The advantages of this DMS-MS method in identification and quantification of GP isomer populations is demonstrated by direct analysis of complex biological extracts without any prior fractionation.

Keywords
lipid isomers, sn-positional isomers, mass spectrometry, differential mobility spectrometry

Disciplines
Medicine and Health Sciences | Social and Behavioral Sciences

Publication Details
Maccarone, A. T., Duldig, J., Mitchell, T. W., Blanksby, S. J., Duchoslav, E. & Campbell, J. Larry. (2014). Characterization of acyl chain position in unsaturated phosphatidylcholines using differential mobility-mass spectrometry. Journal of Lipid Research, 55 (8), 1668-1677.

Authors
Alan Maccarone, Jackson Duldig, Todd W. Mitchell, Stephen J. Blanksby, Eva Duchoslav, and J Campbell

This article was originally published as:
Maccarone, A. T., Duldig, J., Mitchell, T. W., Blanksby, S. J., Duchoslav, E. & Campbell, J. Larry. (2014). Characterization of acyl chain position in unsaturated phosphatidylcholines using differential mobility-mass spectrometry. *Journal of Lipid Research,* 55 (8), 1668-1677.

Rapid and unambiguous characterization of acyl chain position in unsaturated phosphatidylcholines using differential mobility and mass spectrometry

Alan T. Maccarone,[1] Jackson Duldig,[1] Todd W. Mitchell,[2] and Stephen J. Blanksby[3*]

Eva Duchoslav[4] and J. Larry Campbell[4*]

1. School of Chemistry, University of Wollongong, NSW 2522, Australia

2. School of Medicine, University of Wollongong, NSW 2522, Australia

3. Central Analytical Research Facility, Queensland University of Technology, QLD 4000, Australia

4. AB SCIEX, 71 Four Valley Drive, Concord, Ontario, L4K 4V8, Canada

***Corresponding authors:**

stephen.blanksby@qut.edu.au, +61 7 3138 3343 (office), +61 7 3138 4438 (fax)

larry.campbell@absciex.com, +1 289 982 2863 (office), +1 905 660 2623 (fax)

ABSTRACT

Glycerophospholipids that differ in the relative position of the two fatty acyl chains on the glycerol backbone (*i.e.*, *sn*-positional isomers) can have distinct physicochemical properties. The unambiguous assignment of acyl chain position to an individual glycerophospholipid represents a significant analytical challenge. Here we describe a workflow where phosphatidylcholines (PCs) are subjected to electrospray ionization for characterization by a combination of differential mobility spectrometry and mass spectrometry (DMS-MS). When infused as a mixture, ions formed from silver-adduction of each phospholipid isomer (*e.g.*, [PC (16:0/18:1) + Ag]$^+$ and [PC (18:1/16:0) + Ag]$^+$), are transmitted through the DMS device at discrete compensation voltages. Varying their relative amount allows facile and unambiguous assignment of the *sn*-positions of the fatty acyl chains for each isomer. Integration of the well-resolved ion populations provides a rapid method (< 3 mins) for relative quantification of these lipid isomers. The DMS-MS results show excellent agreement with established, but time-consuming, enzymatic approaches, and also provide superior accuracy to methods that rely on mass spectrometry alone. The advantages of this DMS-MS method in identification and quantification of glycerophospholipid isomer populations is demonstrated by direct analysis of complex biological extracts without any prior fractionation.

Supplementary key words: phosphatidylcholine; lipid isomers; *sn*-positional isomers; differential mobility spectrometry; mass spectrometry

INTRODUCTION

Differences in molecular structure are well understood to profoundly influence the biological function of glycerophospholipids (GPs). Numerous accounts have examined the role of GPs in cellular biochemistries including membrane permeability, protein aggregation and receptor activation (1-6). Mass spectrometry (MS) is a powerful tool for GP structure elucidation and is commonly employed in contemporary lipidomics studies of complex biological extracts. Tandem mass spectrometry that employs collision-induced dissociation (CID) is central to most protocols in modern lipidomics and can identify headgroup class, acyl chain length, and degree of acyl chain unsaturation (7-11). However, there are numerous important structural features of GPs that are not easily discerned by CID including: identification of carbon-carbon double bond position(s); the stereochemistry of carbon-carbon double bonds; and the position of substitution of each acyl chain on the glycerol backbone (*i.e.*, *sn*-position) (9, 12, 13). The inability to discriminate between *sn*-positional isomers, or even to unequivocally exclude the presence of both isomers, is an impediment to our understanding of the roles of these distinct molecular structures in biological systems.

Recent reports point to specific arrangements of acyl chains in GPs being responsible for structural interactions that induce specific activity. This has been noted particularly in the interactions of GPs toward nuclear receptor proteins. For example, Liu *et al.* examined the diurnal variation in fat metabolism in mice and suggested that the phosphatidylcholine, PC (18:0/18:1) and not its isomer PC (18:1/18:0) (where the nomenclature indicates *sn*-1/*sn*-2 positions), acts as a trigger for the mediation of fatty acid breakdown in muscles *via* PPARα signaling (14). Elsewhere, Ingraham and colleagues have reported the crystal structure of the phosphatidylglycerol PG (18:1/16:1) bound to the receptor SF-1 (steroidogenic factor-1)

indicating that GP ligands with this arrangement of acyl chains on the glycerol backbone may be required for the protein to function in steroid synthesis (15). These, and related studies, have used CID to examine the acyl chain composition and glycerol backbone position of the target GPs. Such assignments rely on general trends in the product ion abundances in CID mass spectra and are based on literature precedent (16, 17). In some instances, peak intensity ratios have been shown to reveal the relative amounts of each *sn*-positional isomer by benchmarking against enzymatic hydrolysis methods (18). This is necessary because relative ion abundances in CID spectra are influenced by numerous factors including instrument type and experimental configuration (19). However instrument calibration, which could be used to standardize the instrument response, can be confounded by the difficulty in obtaining isomerically pure GPs. Even synthetic preparations that target GPs with a specific acyl chain configuration can give rise to a significant amount of the alternate *sn*-positional isomer (20). With CID mass spectra often ambiguous for assignment of acyl chain position, separation of isomers prior to MS analysis is desirable. Separation of GP *sn*-positional isomers by conventional reversed-phase liquid chromatography however, is only possible where one of the acyl chains has a high degree of unsaturation (21). In the absence of rapid and definitive methods for the determination of acyl chain position, assigning *sn*-position in GPs is often based on the convention of the more unsaturated acyl chain occupying the *sn*-2 position (see below). This raises concerns that some reported GP structures may be entirely incorrect or ignore the likelihood of both isomers being present in the sample. Indeed, it has recently been suggested that GP notation be modified to reflect whether or not the *sn*-position of the acyl chains has been explicitly determined (22).

Current knowledge of the most common acyl chain distribution patterns within GPs has been developed over the last 40 years and is based primarily on digestion within lipid extracts (or

sub-fractions thereof) by enzymes that hydrolyze the ester moieties at select positions on the glycerol backbone (23). These techniques work well for determining the distribution of different fatty acids at the *sn*-1 and -2 of all GPs in an extract and/or a targeted subclass. Numerous accounts detailing the study of eukaryotic lipids have led to the convention of assigning saturated and unsaturated acyl chains at the *sn*-1 and -2 positions, respectively (24-27). However it should be noted that exceptions to this generality have been documented, such as the "unusual" *sn*-distribution in phosphatidylglycerols from the bacterial strain *M. Gallisepticum* found by Rottem and Markowitz (28) where unsaturated fatty acyl chains were found to be prevalent at the *sn*-1 position.

Enzymatic hydrolysis of complex lipid mixtures generally falls short of allowing *sn*-position assignment for a specific combination of fatty acyl chains within a GP subclass. It follows that structural assignment at this level could be achieved if the target lipid could be purified, or at least the pool of lipids significantly simplified, prior to the enzyme assay. Yoshikawa and co-workers succeeded in this by examining only the lipids selectively bound to bovine heart cytochrome C oxidase upon crystallization (29). From this simplified pool, the GP component was further purified and subjected to both mass spectrometry and phospholipase A_2-catalyzed hydrolysis. This analysis allowed definitive assignment of the acyl chain positions within the phosphatidylglycerol PG (16:0/18:1) associated with the protein. This approach, while definitive in assigning molecular structure to GPs, cannot be universally applied and requires significant sample amounts. Such results serve to highlight the need for a technique that can rapidly and unambiguously assign *sn*-position in GPs on diminishingly small amounts of crude lipid extract.

Gas phase separation of isomeric compounds has been demonstrated using ion mobility spectrometry (IMS) with mixtures of ionized molecules resolved based on several physicochemical properties of the ions including: mass-to-charge ratio; size and shape; and dipole moment (30, 31). In a recent critical evaluation of the current tools for lipidomics some of us have suggested that differentiation of isomeric lipids could be achieved by combining IMS and MS workflows (12), considering different IMS technologies have previously been deployed for lipid analysis (32). For example, Jackson *et al*. successfully separated GP classes using drift tube IMS followed by MS identification (33) while Kim and colleagues showed some resolution of phosphatidylcholines (PCs) based on the degree of unsaturation using travelling-wave IMS (34). To this point however, there have been no reports of the application of IMS to resolving *sn*-positional isomers in GPs. Recently there has been renewed interest in a type of IMS known as differential mobility spectrometry (DMS), which in other compound classes has been shown to achieve separation of structural isomers (35, 36), stereoisomers (37), isotopomers (38), and even tautomers (39). But most germane to the current discussion, Shvartsburg *et al.* used a DMS device coupled to an ion-trap mass spectrometer to resolve the ionized lipid diacylglycerols, DG (16:0/12:0/OH) and DG (16:0/OH/12:0), that differ only in the position of the acyl chains on the glycerol backbone (40). Motivated by this demonstration of rapid gas phase *sn*-positional isomer separation on a planar DMS-MS platform, the workflow described herein was developed for the separation and relative quantitation of *sn*-positional isomeric PCs from complex biological extracts on a commercially available system that couples planar DMS with triple quadrupole ion-trap MS.

MATERIALS AND METHODS

Nomenclature

The shorthand notation for lipids suggested recently by Liebisch and co-workers (22) that builds on prior recommendations (41, 42) is used extensively throughout this manuscript when denoting lipid structure.[a] For example, 1-palmitoyl-2-oleoyl-*sn*-glycero-3-phosphatidylcholine is represented as PC (16:0/18:1), where "PC" represents the phosphatidylcholine subclass of the GP class, the "18:1" indicates the number of carbon atoms:number of double bonds, and its placement after the forward slash assigns the position of esterification specifically at *sn*-2 on the glycerol backbone. Analogously the 16:0 positioning before the forward slash indicates a palmitoyl chain esterified at the *sn*-1 position. Where the assignment of the *sn*-position of the acyl chains is uncertain or a mixture of both possible isomers is present, we have adopted the PC (16:0_18:1) notation (22). The term "regioisomer" is used exclusively in this manuscript to refer to one in a given pair of GP *sn*-positional isomers. Silver-adducted lipids denoted as $[M + Ag]^+$ in this work refer to those formed from the ^{107}Ag isotope unless otherwise specified.

Reagents and Materials

Synthetic PC (16:0/18:1), (18:1/16:0), (16:0/18:0), (18:0/16:0), (18:0/18:1), (18:1/18:0) and (16:0/18:2) were obtained from Avanti Polar Lipids, Inc. (Alabaster, AB, USA). Silver acetate, lithium acetate, glycerol, sodium chloride, tris base, phospholipase A_2 (PLA_2) from honey-bee venom (*Apis mellifera*) and the PC fraction from chicken egg yolk were obtained from Sigma-Aldrich (St. Louis, MO, USA). Analytical grades of ammonium acetate, calcium chloride, dichloromethane, and LC-MS grade methanol were purchased from Thermo Fisher Scientific (Scoresby, VIC, Australia) while distilled deionized water (18 MΩ) was produced in-

house using a Synergy UV purification system (Millipore, North Ryde, NSW, Australia). All chemicals listed above were used without further purification. Bovine (*Bos taurus L.*) brain and kidneys were collected from the Wollondilly Abattoir (Picton, NSW, Australia) immediately following the death of the animals and the lipids were extracted as previously described (43).

Mass Spectrometry

All solutions were prepared for electrospray ionization (ESI) and varied slightly in concentration depending on the experiment. In the positive mode experiments, cow brain and kidney extracts were infused at a concentration of 0.1 μM total lipids in methanol containing 50 μM silver acetate, while the egg yolk PC fraction and synthetic lipid solutions contained 0.05 μM (also in 50 μM silver acetate in methanol). For the assay following enzymatic hydrolysis, the lysophosphatidylcholine (LPC) mixtures contained 0.4 μM total LPC in methanol doped with 5 mM ammonium acetate. Synthetic lipid mixtures and all extracts were made up to 0.05 μM total PC in 45:45:10 dichloromethane:methanol:water containing 12 mM ammonium acetate for use in negative-mode experiments. The flow rate in all cases was 15-20 μL min^{-1}.

A differential mobility spectrometer system (SelexION™, AB SCIEX, Concord, ON) was mounted in the atmospheric pressure region between the sampling orifice of a QTRAP® 5500 system (AB SCIEX) and a TurboV™ ESI source (37, 39). All mass spectral data were acquired and analyzed using Analyst™ software version 1.5.2. The following parameters were set unless noted otherwise. The ESI probe was maintained at 5500 V, with a source temperature of 150 °C, nebulizing gas pressure of 20 psi, and auxiliary gas pressure of 5 psi. Nitrogen was used as the curtain gas (20 psi), resolving gas (0 to 35 psi), and CID target gas with inlet set to 3 (arbitrary units, pressure ~ 3mTorr) for the MS^2 and MS^3 experiments. A constant gas flow in the

DMS cell is achieved by the vacuum pumping of the MS system and the DMS temperature was maintained at 225 °C.

The fundamental mechanisms and general operation of this particular form of DMS have been described elsewhere (31, 37, 39, 44). Typically, the DMS was operated at a fixed optimal separation voltage (SV = 4100 V) while the compensation voltage (CV) was ramped from +9 to +14 V. During each 0.10 V step in CV, data were acquired in either an MS^2 (Enhanced Product Ion, EPI) or MS^3 mode. In either case, 5 scans were summed at each CV step for a total acquisition time of 4 to 5 mins. The resulting ionograms were smoothed once using a Gaussian algorithm with a 1 point width prior to extracting peak areas. Manual integration was necessary in some cases where the signal intensity of a feature was relatively low. In complex extracts where the ions representing [PC (34:2) + $^{109}Ag]^+$ and [PC (34:1) + $^{107}Ag]^+$ are isobaric, isotope corrections were carried out as described in supplementary material (Figure V). In certain experiments, both SV and CV were set for the collection of CID spectra from Q1-isolated precursor ions (*m/z* 866.5 for [PC (16:0_18:1) + $Ag]^+$) and in these cases, data were acquired for 3 mins. In between different samples, the syringe and line were flushed with solvent to eliminate cross-contamination of results, which was verified by observing no analytical signal while sampling a blank solution.

The QTRAP 5500 has been modified for ozone-induced dissociation (OzID) in a similar fashion as described previously (45). Here, a combination collision-induced dissociation/ozone-induced dissociation (CID/OzID) workflow was employed as this has been shown capable of revealing acyl chain *sn*-position in phospholipids (13). Sodiated PC (16:0_18:1) cations were generated by ESI and were selected in Q1 at *m/z* 782.2. These ions were accelerated into q2 (collision energy = 38 eV_{Lab}, *i.e.*, the value set for CE in Analyst^{TM} which corresponds to the

voltage offset between the q0 and q2 rods) where they could fragment upon collisions with target gas consisting of a mixture of N_2, O_3 and O_2. The fragment ions, as well as residual intact PC ions, were then trapped in q2 for 1 s. Product ions from the CID/OzID fragmentation processes were cooled and transferred to Q3, where they were analyzed by mass-selective axial ejection at 10,000 Th s^{-1}. All spectra reported here represent the average over 50 scans, totaling 1 min of acquisition time.

Experiments were also conducted with the QTRAP 5500 employing the MS^3 workflow developed by Ekroos *et al.* to determine relative regioisomeric content of PCs (18). Ions of *m/z* 818.5 corresponding to [PC (16:0_18:1) + $CH_3COO]^-$ were formed during negative ion ESI. The ESI probe was maintained at -4500 V, the source at a temperature of 150 °C, the nebulizing gas pressure at 20 psi, and auxiliary gas pressure at 5 psi. Nitrogen was used as the curtain gas (55 psi) and CID target gas (3, arbitrary units). The CE was set to 30 eV_{Lab} for optimal production of $[M - 15]^-$ ions at *m/z* 744.4, while an excitation amplitude of 0.077 V was used to fragment these ions in the Q3 linear ion trap (46). Product ions were scanned out for mass analysis at 2000 Th s^{-1}. The spectra reported here represent the average over 200 scans totaling 3 mins of acquisition time.

PLA_2-catalyzed hydrolysis

The PLA_2 digestion procedure was based on methods described by Bergmeyer *et al.* and a protocol from Sigma-Aldrich (47, 48). Salt free, lyophilized powder of PLA_2 was dissolved in 1:1 water:glycerol (v:v) containing 75 mM NaCl and 10 mM tris buffer (pH 8.0) to produce a PLA_2 concentration of 0.89 units μL^{-1}. Five mixtures varying in theoretical molar amounts of PC (16:0/18:1) and (18:1/16:0) were prepared in LC-MS grade methanol such that each contained

1.2 mL of 10 μM total PC. These mixtures were prepared from the same stock solutions and at the same five theoretical mole percentages (0, 25, 50, 75 and 100% (PC 18:1/16:0)) as those used for direct MS analyses. Each mixture was divided into three separate aliquots of 400 μL and placed in a 1.5 mL Eppendorf tube (Hamburg, Germany) for drying under nitrogen at 37 °C. Each sample was reconstituted with 100 μL of the PLA_2 solution and 5 μL of aqueous 100 mM $CaCl_2$ solution just prior to complete methanol evaporation from the samples. The resulting aqueous solution of lipids, salts, and enzyme was vortexed at 1400 rpm for 7 mins at room temperature followed by dilution of 50 μL of each sample in a glass vial (Thermo Fisher Scientific) with 5 mM ammonium acetate in LC-MS grade methanol to a final volume of 1 mL for storage at −80 °C.

Following positive ion ESI both MS and precursor ion scans for *m/z* 184.1 were used to assay the relative amount of LPCs formed during PLA_2-assisted hydrolysis. Both scan types were used to verify that the hydrolysis had gone to completion. The MS scans were run once per sample to serve as a check against the precursor ion scans (run in triplicate) in the calculation of relative regioisomeric content. The ESI probe was maintained at 5500 V, with a source temperature of 150 °C, nebulizing gas pressure of 25 psi, auxiliary gas pressure of 20 psi, and curtain gas set to 10 psi. The CE was set to 35 eV_{Lab} and the CID target gas inlet to 9 (~6 mTorr) for the precursor ion experiments. Ions were scanned out of Q3 at 200 Th s^{-1} and 175 spectra were averaged over 5 mins of acquisition time for all samples in each assay.

RESULTS

Differential mobility allows rapid separation of PC *sn*-positional isomers

To investigate the ability of DMS to separate PC regioisomers, a simple mixture of synthetic lipids comprising 50% PC (16:0/18:1) and 50% PC (18:1/16:0) was prepared and analyzed. Initially, this solution was subjected to ESI in positive ion mode to yield ions of *m/z* 760.4, corresponding to formation of $[PC\ (34:1) + H]^+$ ions in the gas phase. This ionic form of the PCs was not amenable to DMS separation even when the separation voltage was maximized at 4100 V and resolving gas was employed to increase the ion residence time in the DMS cell. While the use of chemical modifiers (*e.g.*, polar gases or volatile liquids) has been shown to enhance ion separation in some cases (49, Campbell, J.L., Zhu, M., Hopkins, W.S. Ion-Molecule Clustering in Differential Mobility Spectrometry: Lessons Learned from Tetraalkylammonium Cations and their Isomers. *J. Am. Soc. Mass Spectrom.* **2014**, in press), no separation of the protonated PC regioisomers was achieved when the DMS was operated with several of the more common modifiers including isopropanol, acetone, and acetonitrile (data not shown).

Aside from changing the chemical environment of the DMS cell, alteration of the specific form of an ionized molecule can change its mobility. Silver-adducted PC (34:1) cations were formed in the electrospray ion source when the solutions containing the synthetic PCs were doped with silver acetate. When a solution containing synthetic PC (16:0/18:1) was analyzed under these conditions, two distinct features became visible in the resulting ionogram (Figure 1). These features were observed at compensation voltages (CV) of 10.7 and 12.3 V when scanning this voltage in the DMS and monitoring product ions from CID of *m/z* 866.5 corresponding to the $[PC\ (16:0/18:1) + Ag]^+$ cation (Figure 1a). Some groups have highlighted the difficulties with synthesizing isomerically pure PCs (20) and furthermore analyzing their regioisomeric content

(18). Therefore, it was expected that some amount of PC (18:1/16:0) would be present in the PC (16:0/18:1) sample and hence, the smaller peak at CV = 10.7 V was attributed to this component (Figure 1a). To verify this finding, a solution containing synthetic PC (18:1/16:0) in the presence of silver acetate was infused into the instrument and subjected to the same DMS-MS analysis. The resulting ionogram is shown in Figure 1(b) where the location of two peaks is similar to the trace in Figure 1(a), but the feature at CV = 10.7 V now dominates. The result from repeating the same experiment on a 1:1 mixture of the two synthetic PC regioisomers is shown in Figure 1(c), where near baseline resolution is apparent. The collective data in Figure 1 allow assignment of the peak at CV = 10.7 V to the silver-adducted PC (18:1/16:0) and that at 12.3 V to the PC (16:0/18:1) regioisomer. Interestingly, an analysis of the peak areas corresponding to these two ionogram features reveals that the contribution of the isomeric "impurity" in PC (16:0/18:1) (13%, Figures 1a) is greater than that present in PC (18:1/16:0) (1%, Figure 1b). This finding is consistent with PLA_2 assays (see later) and may reflect a difference in the rates of acyl-chain migration during synthesis.

Separation via DMS afforded the opportunity to examine the CID mass spectrum of each *sn*-positional isomer in isolation. Figures 2(a) and (b) show the MS^2 spectra obtained from the 1:1 mixture of synthetic PC regioisomers with the CV across the DMS cell set to values of 12.3 and 10.7 V, respectively. At these voltages the overall ion current is diminished by 20-fold compared to having the DMS deactivated. Diffusive losses in the DMS cell due to increased resolving gas necessary for separation of these ionized regioisomers account for 4-fold of this reduction. Despite this the excellent signal-to-noise in the tandem mass spectra facilitates analysis. The silver adduct ions of a pure regioisomer fragment *via* loss of the neutral phosphocholine headgroup (−183 Da) to produce the base peak at *m/z* 683.5 in each case under

identical MS conditions. Peaks appearing at *m/z* 525.1 and 551.2 correspond to neutral losses of 282 (FA 18:1) and 256 Da (FA 16:0) from the $[M + Ag - N(CH_3)_3]^+$ (*m/z* 807.4) product ions, respectively. Despite being of low abundance (note the 50 times magnification), the relative intensity ratio between these two peaks is seen to switch between regioisomers, *i.e., m/z* 551.2 dominates for isolated [PC (16:0/18:1) + Ag]$^+$ while *m/z* 525.1 is more abundant for [PC (18:1/16:0) + Ag]$^+$. Importantly, *both* of these product ions are formed from *both sn*-positional isomers. This fact is emphasized by the data shown in Figure 1(c) where the extracted ionogram for each of the *m/z* 525.1 and 551.2 product ions reveals features in the total ionogram for both isomers. Although the neutral loss of fatty acids from the *sn*-1 position dominates, this product channel is not exclusive to an individual regioisomer. This is most easily seen at CV = 12.3 V where losses of fatty acyl chains from each of the *sn*-1 and -2 positions in the isolated [PC (16:0/18:1) + Ag]$^+$ are of similar abundance (Figure 1c). MS^3 protocols which examine relative abundances from CID of primary product ions have also been used to assign acyl chain backbone position in GPs (50). The DMS separation of the isomers afforded the opportunity to examine the selectivity of such fragmentation from isomerically pure ion populations. Subsequent dissociation (*i.e.*, MS^3) of the primary $[M + Ag - 183]^+$ product ion at *m/z* 683.2 was undertaken for each of the isolated $[M + Ag]^+$ regioisomers (Figure 2c and d). Ions at *m/z* 371.3 and 389.3 correspond to $[FA\ 18:1 - H_2O + Ag]^+$ and $[FA\ 18:1 + Ag]^+$ (51), respectively. Although their relative intensity switches between pure isomers, both product ions are present in each spectrum indicating that neither is entirely diagnostic of the isomeric form of the phospholipid.

DMS-based separation enables the relative quantitation of PC *sn*-positional isomers

With these initial demonstrations of the DMS-based separation of PC (16:0/18:1) from

PC (18:1/16:0), the quantitative accuracy of this approach was compared against a range of alternative methods. This was done by first preparing mixtures of synthetic PC (16:0/18:1) and PC (18:1/16:0) in different ratios and dividing these for analysis by one of four methods namely: (i) enzymatic digestion with the enzyme PLA_2; (ii) DMS-MS; (iii) negative ion CID; and (iv) a recently described gas-phase ozonolysis approach.

The relative amounts of synthetic PC (16:0/18:1) and PC (18:1/16:0) were determined in the five mixtures by comparing the relative amounts of the lysophosphatidylcholines LPC (16:0_OH) and LPC (18:1_OH) generated from PLA_2 hydrolysis. Precursor ion scans (*m/z* 184.1) were used to assay the reaction (18) by monitoring the abundance of ion signals at *m/z* 496.4 and 522.4, corresponding to $[LPC\ (16:0\_OH) + H]^+$ and $[LPC\ (18:1\_OH) + H]^+$, respectively. Peak heights were used to calculate the relative percentage of PC (18:1_16:0) regiosiomers. For the DMS workflow, MS^3 spectra recorded during CV scanning were used to generate an ionogram from which the area under each peak was used to calculate the relative percentage of each isomer. The correlation between the two methods is described by the straight-line data fit (Figure 3) where the slope of 1.04 (± 0.04) and y-intercept of 0 (± 3) % indicate excellent agreement between the two workflows. More importantly, these results reveal that there is no need for calibration of the DMS method, as the relative peak areas in the ionogram provide accurate relative abundances of the two regioisomers.

Two previously described MS-based techniques were benchmarked against the enzymatic hydrolysis. The method of Ekroos *et al.* (18) employed MS^3 on $[M + CH_3COO]^-$ precursor ions of PCs in a linear ion-trap mass spectrometer and examined the abundance of product ions arising from ketene neutral losses of the fatty acyl chains from demethylated precursor ions, *e.g.,* $[M - CH_3 - 18:1 + H_2O]^-$ and $[M - CH_3 - 16:0 + H_2O]^-$ for PC (16:0/18:1) and PC(18:1/16:0),

respectively. Under their conditions, the neutral loss of the fatty acyl chain (as a ketene) was found to be specific to the *sn*-2 position on the glycerol backbone and was shown to correlate extremely well with enzymatic hydrolysis (18). This method was adapted here on our linear ion-trap platform (QTRAP 5500) and allowed comparison of relative product ion abundances at *m/z* 480.3 and 506.3 corresponding to $[M - CH_3 - 18:1 + H_2O]^-$ and $[M - CH_3 - 16:0 + H_2O]^-$, respectively (supplementary Figure I(c) and (d)). The results are plotted against the enzymatic hydrolysis data from the same set of samples in Figure 3 and show a slope of 0.79 (± 0.03) and y-intercept 9 (± 2) %. While the agreement is good, the slope obtained reflects a systematic bias varied from that observed by Ekroos *et al.* (18) and perhaps arises from the different mass spectrometer and conditions employed here. The susceptibility of peak intensities to be influenced by instrument type and experimental configuration have previously been highlighted (19) and the results shown here emphasize that such methods require instrument-specific calibration against enzymatic approaches (or others) before reliable quantitation of isomers can be realized.

The second MS-only technique employs CID/OzID for determination of acyl chain position in PCs (45). In this approach, sodium adduct ions of each PC (16:0_18:1) regioisomer at *m/z* 782.2 undergo CID to lose the PC headgroup and form a fragment ion *m/z* 599.2. It is postulated that this unimolecular dissociation is driven by the ester moiety of the *sn*-2 fatty acyl chain and results in a dioxolane ring bearing a newly formed carbon-carbon double bond (supplementary Figure I(a) and (b)) (50). Subsequent OzID at this newly created carbon-carbon double bond yields fragmentation diagnostic for the acyl chain composition at *sn*-2 (*i.e.,* for PC (18:1/16:0) *m/z* 405.0 and 421.1 while for (16:0/18:1) *m/z* 379.0 and 395.0; supplementary Figure I(a) and (b), insets). This mechanism has previously been verified by performing discrete

CID and OzID fragmentation experiments on a single-stage linear ion trap on the same batch of synthetic PCs explored here (13). The CID/OzID results obtained in the present study correlate well with the PLA_2 hydrolysis; however, the slope of 0.94 (± 0.03) and y-intercept 4 (± 2) % suggest a small correction is needed. This small systematic variation in the slope may reflect the contribution from an alternate fragmentation pathway from *m/z* 782.2 to 599.2 (13).

Rapid quantitation of PC *sn*-positional isomers from complex biological matrices

Three complex lipid extracts were also analyzed: (i) PC fraction from chicken egg yolk; as well as the total lipid extracts from (ii) cow brain and (iii) cow kidney. Each diluted extract solution was subjected to electrospray ionization in the presence of silver acetate for analysis via the DMS-MS workflow described above. The results are shown in Figure 4 where, in each of the extracts examined, two features are present with the same CV values as those for the synthetic PC (34:1) regioisomers (Figure 1). Each experiment required 4.5 mins of acquisition time – a mere fraction of the typical run times needed by traditional analyses.

The area under the curves in Figure 4 allows relative regioisomeric quantification of the PC (34:1) component within these complex biological samples. Chicken egg yolk was found to be more enriched in the PC (16:0/18:1) regioisomer than even the commercially available synthetic lipid. For the two bovine organs studied, the relative proportions of the two regioisomers varies by a factor of two, emphasizing a varying isomeric distribution between organs of this particular mammal. Precedent for this observation has been reported by Pham *et al.* who showed similar changes in isomer ratios for the same tissues using the MS-based CID/OzID technique (13); and by Taguchi and co-workers who showed the relative amounts of PC (16:0_22:6) regioisomers varied significantly between brain and liver tissues in mice (21).

Factors influencing DMS separation of PC *sn*-positional isomers

Ultimately, the successful DMS-based separation of PC (16:0/18:1) from PC (18:1/16:0) was afforded by three key factors: (i) cationization of the PCs with silver, (ii) the presence of a carbon-carbon double bond on an acyl chain of the PC, and (iii) use of resolving gas to enhance resolution. To examine the effect of the cation type for the separation of the PC regioisomers, we generated several different forms of the ionized lipids by electrospray ionization, including the protonated form and several metal cation adducts with the formula $[M + X]^+$, where X = Li^+, Na^+, K^+, or Ag^+. Upon examination, only the silver-adduct ions of PCs were separable by DMS (Figure 5a). While the Li^+ adducts appeared to demonstrate some degree of separation, it required more rigorous DMS conditions that resulted in greater signal depletion. The need for silver in the successful separation of these regioisomers might arise from the known abilities of this metal ion to bind not only to lone pairs of electrons present on heteroatoms (like O and N), but also to π-electrons present in carbon-carbon multiple bonds, such as the alkene group present in one acyl chain of the PCs studied here (52).

It was clear that the presence of the silver cation was critical to the ability to separate the two PC regioisomers by DMS. Given the ability for silver to coordinate with carbon-carbon double bonds, the potential role of the carbon-carbon double bond on the oleoyl chain was investigated. Similar DMS-based analysis was conducted on a related pair of regioisomeric lipids each of which has fully saturated acyl chains: PC (16:0/18:0) and PC (18:0/16:0). As shown in supplementary Figure II, no DMS-based separation of $[M + Ag]^+$ regioisomers from a 1:1 mixture of PC (16:0/18:0) and PC (18:0/16:0) containing silver acetate was achieved using conditions that separated PC (16:0/18:1) from PC (18:1/16:0). This result suggests that the carbon-carbon double bond present in the latter pair plays an integral role in the DMS-based

separation of these PC regioisomers. This is supported by other research results inferring silver affinity for carbon-carbon double bonds in both the liquid and gas phases (51-53). A 1:1 mixture of PC (18:0/18:1) with PC (18:1/18:0) was also subjected to the same workflow in order to examine the effect of chain length on separation (supplementary Figure III). The results indicate that this mixture of regioisomers, where both acyl chains have identical length, can also be well separated by DMS provided at least one of the chains is unsaturated.

The standard residence time for the PC ions within the DMS cell (~7 ms) was not sufficient to separate the silver-adducted PC (16:0_18:1) regioisomers during CV voltage scanning. However, we could extend the residence time for these ions by introducing an impeding gas flow from the terminus of the DMS cell (*i.e.*, in between the DMS cell and the orifice where ions enter the MS). As indicated in Figure 5(b) for the $[M + Ag]^+$ ions, no separation was observed for resolving gas pressures up to 20 psi. However, when the resolving gas pressure was increased to 25 psi, two features at 10.7 and 12.3 V in CV space emerged. Further increasing the resolving gas pressure to 35 psi provided clear separation of the two regioisomeric lipid ions. The need for additional residence time (*ca.* 12 ms when resolving gas pressure was 35 psi) to separate these ion populations suggests subtle structural differences between these two regioisomeric ions in the gas phase.

DISCUSSION

The DMS-MS workflow developed here provides for unambiguous differentiation of *sn*-positional isomers of unsaturated PCs and is compatible with both liquid chromatography- and direct infusion-MS protocols (8, 9, 11). The amount of sample and preparation time required for this method are significantly reduced when compared to those involving enzymatic hydrolysis of

glycerophospholipids (24, 54). Furthermore, the relative quantitation of PC regioisomers obtained by DMS-MS shows excellent agreement with values derived from these well-established wet chemical assays. The demonstration that isomeric forms of ionized lipids can be well separated in the gas phase indicates that calibration against classical methods is not required and thus presents a significant advantage over methods relying on mass spectrometry alone.

The separation of PC (16:0/18:1) from PC (18:1/16:0) as silver-adducted ions has allowed interrogation of the fragmentation processes associated with each isomer in isolation. Given the difficulty in obtaining a single GP isomer from either synthetic or biological sources, the tandem mass spectra presented here may be among the first obtained from an isomerically pure lipid. These data reveal that while the abundance of product ions arising from ionized forms of PC are affected by the substitution pattern on the glycerol backbone, no single product ion is found to be an exclusive indicator of *sn*-position. Rather these results reflect competition amongst dissociation pathways (*e.g.*, neutral losses from *sn*-1 and *sn*-2 positions) even within a single GP isomer. Indeed, it has recently been shown that for related ionized glycerolipids (*i.e.*, triacylglycerols) the energetic and entropic dependence of the dissociation pathways are a function of the *sn*-positional distribution (55). The existence of competing pathways for dissociation is consistent with the observations that: (i) product ions arising from competing dissociation pathways are affected by instrument configuration and experimental parameters (19); and (ii) under typical instrument conditions product ions are not exclusive to a particular isomer. Taken together, this suggests that tandem mass spectrometric techniques that examine peak abundances alone, and in the absence of calibration, should not be used to assign a single acyl chain substitution pattern in GPs. Instead, product ion abundances should be used as a guide to indicate *only the most abundant isomer* present in the sample.

Where mass spectral data provide the GP class and the stoichiometry of the two acyl chains the assignment of fatty acyl chain position on the glycerol backbone is sometimes undertaken using rules of thumb (*e.g.*, the more unsaturated chain is at the *sn*-2 position). It is worth remembering that the precedents for these conventions derive from enzymatic assays conducted on lipid extracts or class fractions and are thus insensitive to relative populations of each pair of regioisomers. The data presented here, along with previous studies (18, 21), demonstrate that in biological extracts GPs are most often present as a mixture of both regioisomers. As such, assignment of the structure exclusively to one isomer based on convention alone may be entirely incorrect or serve to mask the true molecular diversity of the lipidome. We thus support the recent suggestion of Liebisch *et al.* that the notation for lipid structural assignment should precisely reflect the information provided by the specific analyses undertaken (*e.g.*, PC (16:0_18:1) where the *sn*-positions are not explicitly determined) (22).[a]

Results described herein demonstrate that the degree of unsaturation and the ionized form of a particular PC (*i.e.*, $[PC + X]^+$ where X = Na, Li, Ag) influence the resolving power of the planar DMS cell employed here. Using this protocol, at least one degree of unsaturation is required to separate *sn*-positional isomers and, of the metal ions investigated, only silver adduct ions were found to provide sufficient separation for quantitative workflows. In considering the scope of this approach, DMS conditions were also optimized to induce separation of regioisomeric forms of the representative polyunsaturated lipid PC(16:0_18:2) (see supplemental Figure IV). Future efforts to optimize and benchmark the DMS-MS approach for other PC isomers or other classes of glycerolipids would be greatly assisted by increased availability of pairs of synthetic isomers. The use of silver adducts was found to be effective for increasing the resolving power of the DMS method by analogy with traditional silver ion-chromatographic

approaches (52, 53). The presence of two abundant silver isotopes separated in mass by 2 Da does introduce some complexity to the analysis but methods to account for these isobars in quantitative workflows are demonstrated here (see supplemental Figure V) and are similar to approaches already used for isotope corrections in low resolution shotgun lipidomics protocols. As the theory of DMS further evolves, it is expected that the scope of this approach for the analysis of isomeric lipids will expand to encompass a broader range of lipid classes and may enable its use with a wider variety of ion types.

Even within the scope of lipids presented here, the ability of DMS to filter for a targeted lipid regioisomer represents a significant advance towards the goal of total lipid structure elucidation within the complex molecular makeup of a crude biological extract. The precise molecular information afforded by this approach could play a critical role in understanding which individual lipid molecules are responsible for particular cellular functions. Further structural motif identification, *i.e.,* double bond location and stereochemistry, may be possible in the near future when DMS is coupled with other MS methods. The work here builds on previous effort examining the ion mobility of lipids (32) and supports the idea that coupling mobility with MS may produce powerful tools for application towards total structure elucidation within the field of lipidomics (12).

ACKNOWLEDGMENTS

We extend our thanks to the following people for their assistance in the development of the enzymatic hydrolysis procedure and subsequent assay implemented here: Prof. Nick Dixon (UOW) and his group members Dr. Zhi-Qiang Xu and Mr. Nicholas Horan; Drs. Simon Brown (UOW) and Kim Ekroos (Zora Biosciences, Finland). We also acknowledge Dr. Jessica Hughes (UOW) for providing the bovine organ lipid extracts. J.L.C. would like to thank Drs. Yves Le Blanc and Jim Hager for insightful discussions regarding the mobility experiments. S.J.B. and T.W.M. are grateful to the Australian Research Council (ARC) and AB SCIEX for support of this research through the Linkage scheme (LP110200648). T.W.M. is an ARC Future Fellow (FT110100249) and S.J.B. is supported by the ARC Centre of Excellence for Free Radical Chemistry and Biotechnology (CE0561607).

REFERENCES

1. Gurr, M. I., J. L. Harwood, and K. N. Frayn. 2002. Lipid Biochemistry, Blackwell Science, Oxford. 215-263.

2. Lee, A. 2001. Membrane structure. *Curr. Biol.* **11**: R811-R814.

3. Janmey, P. A., and P. K. J. Kinnunen. 2006. Biophysical properties of lipids and dynamic membranes. *Trends Cell Biol.* **16**: 538-546.

4. Gross, R. W., C. M. Jenkins, J. Y. Yang, D. J. Mancuso, and X. L. Han. 2005. Functional lipidomics: the roles of specialized lipids and lipid-protein interactions in modulating neuronal function. *Prostaglandins Other Lipid Mediat.* **77**: 52-64.

5. Menon, A. K. 2008. Lipid Modifications of Proteins. *In* Biochemistry of Lipids, Lipoproteins and Membranes. D. E. Vance and J. E. Vance, editors. Elsevier, Sydney. 39-58.

6. Dowhan, W., M. Bogdanov, and E. Mileykovskaya. 2008. Functional roles of lipids in membranes. *In* Biochemistry of Lipids, Lipoproteins, and Membranes. D. E. Vance and J. E. Vance, editors. Elsevier, Sydney. 1-37.

7. Brügger, B., G. Erben, R. Sandhoff, F. T. Wieland, and W. D. Lehmann. 1997. Quantitative analysis of biological membrane lipids at the low picomole level by nano-electrospray ionization tandem mass spectrometry. *Proc. Natl. Acad. Sci. USA* **94**: 2339-2344.

8. Han, X., K. Yang, and R. W. Gross. 2012. Multi-dimensional mass spectrometry-based shotgun lipidomics and novel strategies for lipidomic analyses. *Mass. Spectrom. Rev.* **31**: 134-178.

9. Blanksby, S. J., and T. W. Mitchell. 2010. Advances in Mass Spectrometry for Lipidomics. *Ann. Rev. Anal. Chem.* **3**: 433-465.

10. Shevchenko, A., and K. Simons. 2010. Lipidomics: coming to grips with lipid diversity. *Nat. Rev. Mol. Cell Biol.* **11**: 593-598.

11. Pulfer, M., and R. C. Murphy. 2003. Electrospray mass spectrometry of phospholipids. *Mass. Spectrom. Rev.* **22**: 332-364.

12. Brown, S. H. J., T. W. Mitchell, A. J. Oakley, H. T. Pham, and S. J. Blanksby. 2012. Time to Face the Fats: What Can Mass Spectrometry Reveal about the Structure of Lipids and Their Interactions with Proteins? *J. Am. Soc. Mass Spectrom.* **23**: 1441-1449.

13. Pham, H. T., A. T. Maccarone, M. C. Thomas, J. L. Campbell, T. W. Mitchell, and S. J. Blanksby. 2014. Structural characterization of glycerophospholipids by combinations of ozone- and collision-induced dissociation mass spectrometry: the next step towards "top-down" lipidomics. *Analyst* **139**: 204-214.

14. Liu, S., J. D. Brown, K. J. Stanya, E. Homan, M. Leidl, K. Inouye, P. Bhargava, M. R. Gangl, L. Dai, B. Hatano, G. S. Hotamisligil, A. Saghatelian, J. Plutzky, and C.-H. Lee. 2013. A diurnal serum lipid integrates hepatic lipogenesis and peripheral fatty acid use. *Nature* **502**: 550-554.

15. Krylova, I. N., E. P. Sablin, J. Moore, R. X. Xu, G. M. Waitt, J. A. MacKay, D. Juzumiene, J. M. Bynum, K. Madauss, V. Montana, L. Lebedeva, M. Suzawa, J. D. Williams, S. P. Williams, R. K. Guy, J. W. Thornton, R. J. Fletterick, T. M. Willson, and H. A. Ingraham. 2005. Structural analyses reveal phosphatidyl inositols as ligands for the NR5 orphan receptors SF-1 and LRH-1. *Cell* **120**: 343-355.

16. Hsu, F.-F., and J. Turk. 2009. Electrospray ionization with low-energy collisionally activated dissociation tandem mass spectrometry of glycerophospholipids: Mechanisms of fragmentation and structural characterization. *J. Chromatogr. B* **877**: 2673-2695.

17. Huang, Z. H., D. A. Gage, and C. C. Sweeley. 1992. Characterization of diacylglycerylphosphocholine molecular species by FAB-CAD-MS/MS: a general method not sensitive to the nature of the fatty acyl groups. *J. Am. Soc. Mass Spectrom.* **3**: 71-78.

18. Ekroos, K., C. S. Ejsing, U. Bahr, M. Karas, K. Simons, and A. Shevchenko. 2003. Charting molecular composition of phosphatidylcholines by fatty acid scanning and ion trap MS3 fragmentation. *J. Lipid Res.* **44**: 2181-2192.

19. Hou, W., H. Zhou, M. B. Khalil, D. Seebun, S. A. L. Bennett, and D. Figeys. 2011. Lyso-form fragment ions facilitate the determination of stereospecificity of diacyl glycerophospholipids. *Rapid Commun. Mass Spectrom.* **25**: 205-217.

20. Plückthun, A., and E. A. Dennis. 1982. Acyl and phosphoryl migration in lysophospholipids: importance in phospholipid synthesis and phospholipase specificity. *Biochem.* **21**: 1743-1750.

21. Nakanishi, H., Y. Iida, T. Shimizu, and R. Taguchi. 2010. Separation and quantification of sn-1 and sn-2 fatty acid positional isomers in phosphatidylcholine by RPLC-ESIMS/MS. *J. Biochem.* **147**: 245-256.

22. Liebisch, G., J. A. Vizcaíno, H. Köfeler, M. Trötzmüller, W. J. Griffiths, G. Schmitz, F. Spener, and M. J. O. Wakelam. 2013. Shorthand notation for lipid structures derived from mass spectrometry. *J. Lipid Res.* **54**: 1523-1530.

23. Stern, W., and M. E. Pullman. 1978. Acyl-CoA-sn-glycerol-3-phosphate acyltransferase and positional distribution of fatty acids in phospholipids of cultured cells. *J. Biol. Chem.* **253**: 8047-8055.

24. Kielbowicz, G., W. Gladkowski, A. Chojnacka, and C. Wawrzenczyk. 2012. A simple method for positional analysis of phosphatidylcholine. *Food Chem.* **135**: 2542-2548.

25. Connor, W. E., D. S. Lin, G. Thomas, F. Ey, T. DeLoughery, and N. Zhu. 1997. Abnormal phospholipid molecular species of erythrocytes in sickle cell anemia. *J. Lipid Res.* **38**: 2516-2528.

26. Van Deenen, L. L. 1971. Chemistry of phospholipids in relation to biological membranes. *Pure Appl. Chem.* **25**: 25-56.

27. Lands, W. E. M. 2000. Stories about acyl chains. *Biochim. Biophys. Acta* **1483**: 1-14.

28. Rottem, S., and O. Markowitz. 1979. Membrane lipids of *Mycoplasma gallisepticum*: a disaturated phosphatidylcholine and a phosphatidylglycerol with an unusual positional distribution of fatty acids. *Biochem.* **18**: 2930-2935.

29. Shinzawa-Itoh, K., H. Aoyama, K. Muramoto, H. Terada, T. Kurauchi, Y. Tadehara, A. Yamasaki, T. Sugimura, S. Kurono, K. Tsujimoto, T. Mizushima, E. Yamashita, T. Tsukihara, and S. Yoshikawa. 2007. Structures and physiological roles of 13 integral lipids of bovine heart cytochrome c oxidase. *EMBO J.* **26**: 1713-1725.

30. Kanu, A. B., P. Dwivedi, M. Tam, L. Matz, and H. H. Hill Jr. 2008. Ion mobility-mass spectrometry. *J. Mass Spectrom.* **43**: 1-22.

31. Eiceman, G. A., and Z. Karpas. 2005. Ion Mobility Spectrometry, CRC Press, Boca Raton

32. Kliman, M., J. C. May, and J. A. McLean. 2011. Lipid analysis and lipidomics by structurally selective ion mobility-mass spectrometry. *Biochim. Biophys. Acta* **1811**: 935-945.

33. Jackson, S. N., M. Ugarov, J. D. Post, T. Egan, D. Langlais, J. A. Schultz, and A. S. Woods. 2008. A study of phospholipids by ion mobility TOF/MS. *J. Am. Soc. Mass Spectrom.* **19**: 1655-1662.

34. Kim, H. I., H. Kim, E. S. Pang, E. K. Ryu, L. W. Beegle, J. A. Loo, W. A. Goddard, and I. Kanik. 2009. Structural Characterization of Unsaturated Phosphatidylcholines Using Traveling Wave Ion Mobility Spectrometry. *Anal. Chem.* **81**: 8289-8297.

35. Barnett, D. A., B. Ells, R. Guevremont, and R. W. Purves. 1999. Separation of leucine and isoleucine by electrospray ionization-high field asymmetric waveform ion mobility spectrometry-mass spectrometry. *J. Am. Soc. Mass Spectrom.* **10**: 1279-1284.

36. Blagojevic, V., A. Chramow, B. B. Schneider, T. R. Covey, and D. K. Bohme. 2011. Differential mobility spectrometry of isomeric protonated dipeptides: modifier and field effects on ion mobility and stability. *Anal. Chem.* **83**: 3470-3476.

37. Schneider, B. B., T. R. Covey, S. L. Coy, E. V. Krylov, and E. G. Nazarov. 2010. Planar differential mobility spectrometer as a pre-filter for atmospheric pressure ionization mass spectrometry. *Int. J. Mass. Spectrom.* **298**: 45-54.

38. Shvartsburg, A. A., D. E. Clemmer, and R. D. Smith. 2010. Isotopic Effect on Ion Mobility and Separation of lsotopomers by High-Field Ion Mobility Spectrometry. *Anal. Chem.* **82**: 8047-8051.

39. Campbell, J. L., J. C. Y. Le Blanc, and B. B. Schneider. 2012. Probing Electrospray Ionization Dynamics Using Differential Mobility Spectrometry: The Curious Case of 4-Aminobenzoic Acid. *Anal. Chem.* **84**: 7857-7864.

40. Shvartsburg, A. A., G. Isaac, N. Leveque, R. D. Smith, and T. O. Metz. 2011. Separation and Classification of Lipids Using Differential Ion Mobility Spectrometry. *J. Am. Soc. Mass Spectrom.* **22**: 1146-1155.

41. Fahy, E., S. Subramaniam, H. A. Brown, C. K. Glass, A. H. Merrill, R. C. Murphy, C. R. H. Raetz, D. W. Russell, Y. Seyama, W. Shaw, T. Shimizu, F. Spener, G. van Meer, M. S.

VanNieuwenhze, S. H. White, J. L. Witztum, and E. A. Dennis. 2005. A comprehensive classification system for lipids. *J. Lipid Res.* **46**: 839-861.

42. Fahy, E., S. Subramaniam, R. C. Murphy, M. Nishijima, C. R. H. Raetz, T. Shimizu, F. Spener, G. van Meer, M. J. O. Wakelam, and E. A. Dennis. 2009. Update of the LIPID MAPS comprehensive classification system for lipids. *J. Lipid Res.* **50**: S9-S14.

43. Nealon, J. R., S. J. Blanksby, T. W. Mitchell, and P. L. Else. 2008. Systematic differences in membrane acyl composition associated with varying body mass in mammals occur in all phospholipid classes: an analysis of kidney and brain. *J. Exp. Biol.* **211**: 3195-3204.

44. Shvartsburg, A. A. 2009. Differential Ion Mobility Spectrometry: Nonlinear Ion Transport and Fundamentals of FAIMS, CRC Press, Boca Raton. 1-293.

45. Poad, B. L. J., H. T. Pham, M. C. Thomas, J. R. Nealon, J. L. Campbell, T. W. Mitchell, and S. J. Blanksby. 2010. Ozone-Induced Dissociation on a Modified Tandem Linear Ion-Trap: Observations of Different Reactivity for Isomeric Lipids. *J. Am. Soc. Mass Spectrom.* **21**: 1989-1999.

46. Collings, B. A., and M. A. Romaschin. 2009. MS/MS of Ions in a Low Pressure Linear Ion Trap using a Pulsed Gas. *J. Am. Soc. Mass Spectrom.* **20**: 1714-1717.

47. Bergmeyer, H. U., M. Graßl, and W. Hans-Elmar. 1983. Enzymes. *In* Methods of Enzymatic Analysis. H. U. Bergmeyer, editor. Verlag Chemie, Basel. 283-284.

48. Sigma-Aldrich. 1993. Enzymatic Assay of Phospholipase A2 (EC 3.1.1.4).

49. Schneider, B. B., T. R. Covey, S. L. Coy, E. V. Krylov, and E. G. Nazarov. 2010. Chemical Effects in the Separation Process of a Differential Mobility/Mass Spectrometer System. *Anal. Chem.* **82**: 1867-1880.

50. Hsu, F. F., and J. Turk. 2003. Electrospray ionization/tandem quadrupole mass spectrometric studies on phosphatidylcholines: The fragmentation processes. *J. Am. Soc. Mass Spectrom.* **14**: 352-363.

51. Yoo, H. J., and K. Hakansson. 2011. Determination of Phospholipid Regiochemistry by Ag(I) Adduction and Tandem Mass Spectrometry. *Anal. Chem.* **83**: 1275-1283.

52. Damyanova, B., S. Momtchilova, S. Bakalova, H. Zuilhof, W. W. Christie, and J. Kaneti. 2002. Computational probes into the conceptual basis of silver ion chromatography: I. Silver(I) ion complexes of unsaturated fatty acids and esters. *J. Mol. Struct. (Theochem)* **589-590**: 239-249.

53. Morris, L. J. 1966. Separations of lipids by silver ion chromatography. *J. Lipid Res.* **7**: 717-732.

54. Chen, S., and P. V. Subbaiah. 2013. Regioisomers of Phosphatidylcholine Containing DHA and Their Potential to Deliver DHA to the Brain: Role of Phospholipase Specificities. *Lipids* **48**: 675-686.

55. Renaud, J. B., S. Overton, and P. M. Mayer. 2013. Energy and entropy at play in competitive dissociations: The case of uneven positional dissociation of ionized triglycerides. *Int. J. Mass. Spectrom.* **352**: 77-86.

FOOTNOTES

Titlepage

Abbreviations: PC, phosphatidylcholine; DMS, differential mobility spectrometry; MS, mass spectrometry; GP, glycerophospholipid; CID, collision-induced dissociation; SF-1, steroidogenic factor-1; IMS, ion mobility spectrometry; DG, diacylglycerol; PLA_2, phospholipase A_2; LPC, lysophosphatidylcholine; CV, compensation voltage; OzID, ozone-induced dissociation; CID/OzID, collision-induced dissociation/ozone-induced dissociation; CE, collision energy.

Pages 7 & 21

[a] Liebisch and co-workers do not recommend the use of parentheses unless specifying double bond position and stereochemistry within a specific acyl chain (reference 22). In this manuscript we stray from this recommendation and use parentheses to encapsulate a given *sn*-1 and -2 acyl chain pair to aid distinction between frequently mentioned *sn*-positional isomers.

FIGURES and CAPTIONS

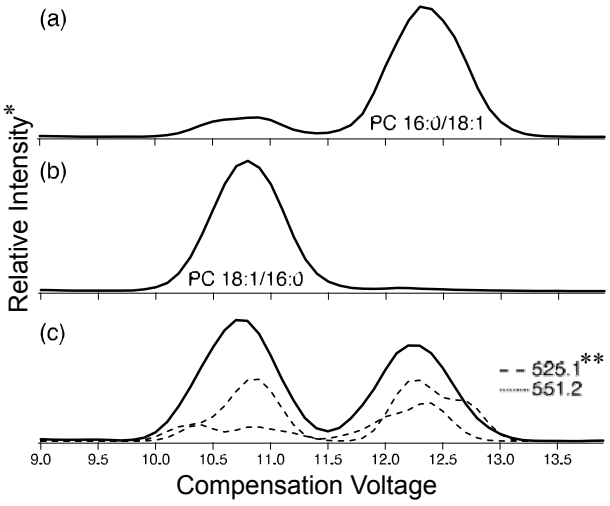

Figure 1. Total ionograms resulting from differential mobility spectrometry-based separation of [PC (16:0_18:1) + Ag]$^+$ *sn*-positional isomers formed during positive-mode electrospray ionization of silver acetate-doped solutions of synthetic lipids (a) PC (16:0/18:1), (b) PC (18:1/16:0) and (c) a 1:1 mixture of the two. *Relative intensity represents the total ion abundance resulting from collision-induced dissociation of *m/z* 866.5 [M + Ag]$^+$ ions. The dashed lines (** both magnified 50 times) are extracted ionograms and represent the ion abundance for *m/z* 525.1 and 551.2 product ions.

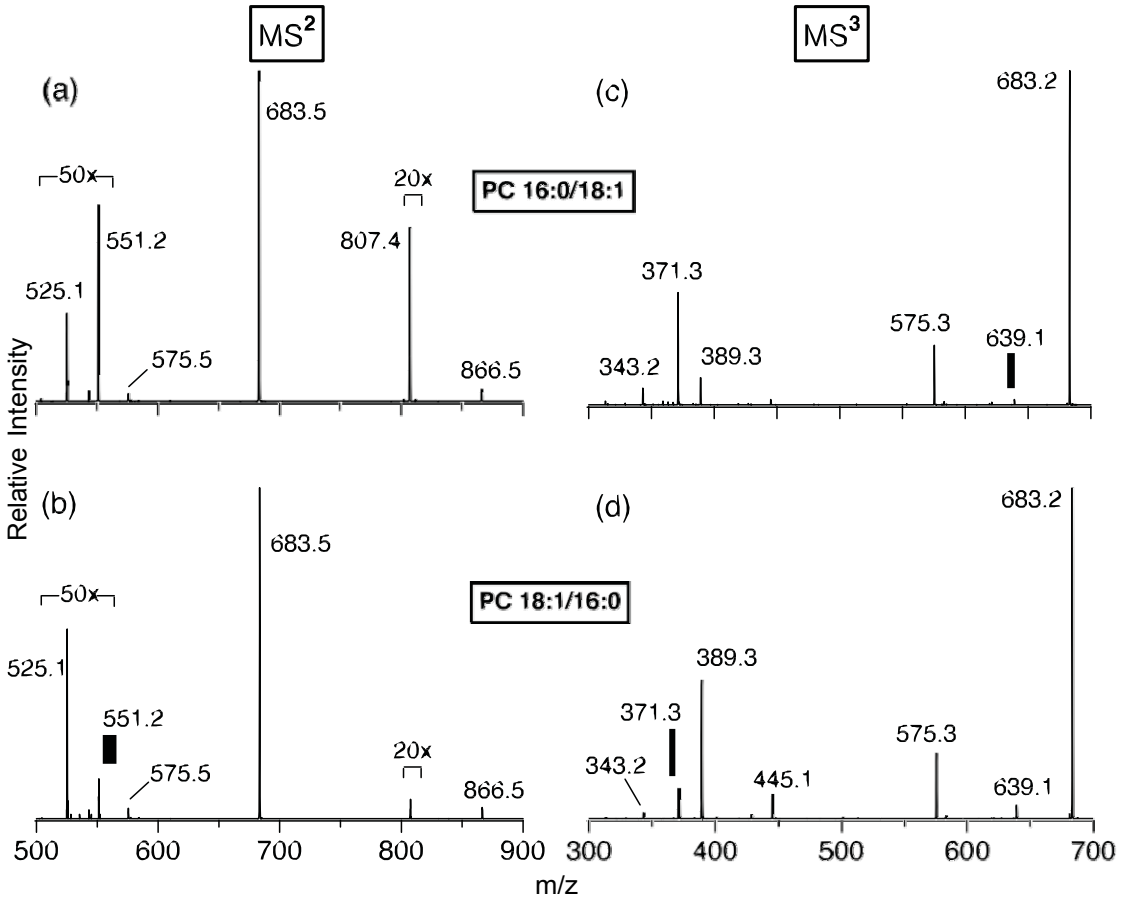

Figure 2. Collision-induced dissociation (CID) spectra recorded following differential mobility spectrometry-based isolation of [PC (16:0/18:1) + Ag]$^+$ with compensation voltage set to 12.3 V (panels a and c) or [PC (18:1/16:0) + Ag]$^+$ with compensation voltage set to 10.7 V (panels b and d); ions were formed from electrospray ionization of a 1:1 mixture of the two *sn*-positional isomers in the presence of silver acetate. The MS^2 spectra (a and b) show product ions from CID of *m/z* 866.5 [M + Ag]$^+$ ions while the MS^3 spectra (c and d) show subsequent products from CID of *m/z* 683.2 [M + Ag − 183]$^+$ ions.

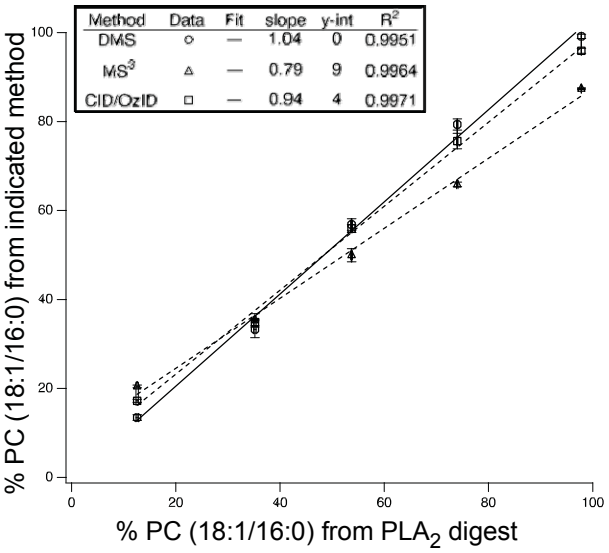

Figure 3. Graph showing the correlation of each indicated method (ordinate) with the PLA_2 digestion (abscissa) performed on five regioisomeric mixtures of PC (16:0_18:1). The errors bars in x are from propagating the standard deviation in the mean of three replicates across three sample sets and are less than 0.25% PC (18:1/16:0). Those in y are from the standard deviation in the mean of three replicates and are less than 2% PC (18:1/16:0).

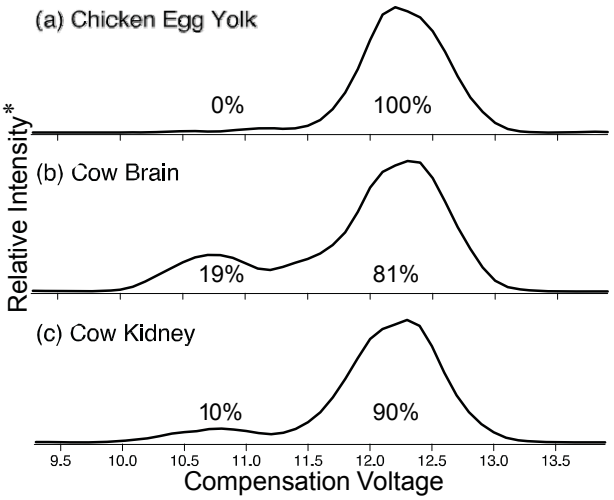

Figure 4. Total ionograms resulting from differential mobility spectrometry-based separation of [PC (16:0_18:1) + Ag]$^+$ *sn*-positional isomers formed during positive-mode electrospray ionization of lipid extracts from each of the indicated biological samples in the presence of silver acetate. *Relative Intensity represents the total ion abundance resulting from collision-induced dissociation of *m/z* 683.2 [M + Ag − 183]+ ions. The listed percentages (± 4 from the error in the slope of the solid trace in Figure 3) are the relative amounts from peak integration following correction for isobaric contribution from [PC (16:0_18:2) + ^{109}Ag]$^+$ present in each extract (see supplemental Figure V).

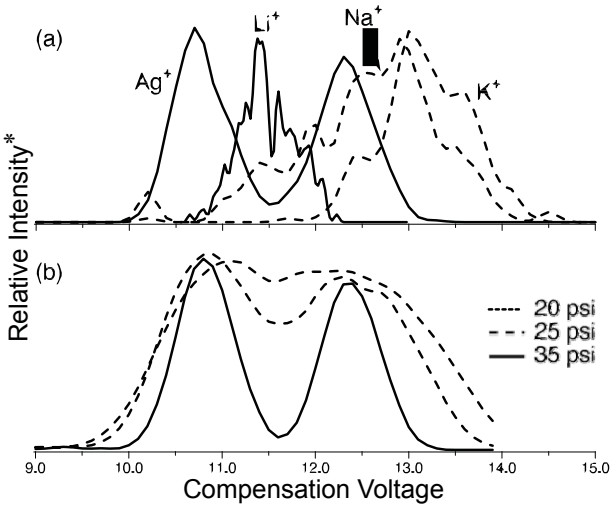

Figure 5. The effect on the $[M + X]^+$ regioisomeric separation capability in the differential mobility spectrometer of (a) X in a 1:1 mixture of PC (16:0/18:1) and (18:1/16:0), and (b) resolving gas pressure in a 1:1 mixture of PC (16:0/18:1) and (18:1/16:0) with X = Ag^+. *Relative Intensity in each trace in panel (a) represents the extracted ion abundance for those products corresponding to neutral loss of 183 Daltons from collision-induced dissociation (CID) of $[M + X]^+$ ions. Each trace in panel (b) represents the total ion abundance resulting from CID of *m/z* 866.5 $[M + Ag]^+$ ions. In both panels the data has been approximately normalized to the respective solid black trace.